Infrared light-emitting diodes based on colloidal PbSe/PbS core/shell nanocrystals*

Byung-Ryool Hyun[1], Mikita Marus[1], Huaying Zhong(钟华英)[1], Depeng Li(李德鹏)[1], Haochen Liu(刘皓宸)[1], Yue Xie(谢阅)[1], Weon-kyu Koh[2], Bing Xu(徐冰)[1,3], Yanjun Liu(刘言军)[1], and Xiao Wei Sun(孙小卫)[1,3,†]

[1] *Guangdong University Key Laboratory for Advanced Quantum Dot Displays and Lighting, Shenzhen Key Laboratory for Advanced Quantum Dot Displays and Lighting, Department of Electrical & Electronic Engineering, Southern University of Science and Technology, Shenzhen* 518055, *China*

[2] *School of Electrical and Electronic Engineering, Nanyang Technological University, Singapore*

[3] *Shenzhen Planck Innovation Technologies Co. Ltd, Shenzhen* 518112, *China*

(Received 16 October 2019; revised manuscript received 26 November 2019; accepted manuscript online 9 December 2019)

Colloidal PbSe nanocrystals (NCs) have gained considerable attention due to their efficient carrier multiplication and emissions across near-infrared and short-wavelength infrared spectral ranges. However, the fast degradation of colloidal PbSe NCs in ambient conditions hampers their widespread applications in infrared optoelectronics. It is well-known that the inorganic thick-shell over core improves the stability of NCs. Here, we present the synthesis of PbSe/PbS core/shell NCs showing wide spectral tunability, in which the molar ratio of lead (Pb) and sulfur (S) precursors, and the concentration of sulfur and PbSe NCs in solvent have a significant effect on the efficient PbS shell growth. The infrared light-emitting diodes (IR-LEDs) fabricated with the PbSe/PbS core/shell NCs exhibit an external quantum efficiency (EQE) of 1.3 % at 1280 nm. The ligand exchange to optimize the distance between NCs and chloride treatment are important processes for achieving high performance on PbSe/PbS NC-LEDs. Our results provide evidence for the promising potential of PbSe/PbS NCs over the wide range of infrared optoelectronic applications.

Keywords: PbSe/PbS core/shell nanocrystal, ligand exchange, infrared light-emitting diodes, external quantum efficiency

PACS: 85.60.Jb, 85.60.Bt, 61.46.Df, 61.46.Hk **DOI:** 10.1088/1674-1056/ab5fb7

1. Introduction

Infrared light-emitting diodes (IR-LEDs) and lasers have been widely used for a variety of practical applications including short- or long-range communications, medical diagnostics, and security.[1–3] Recently, near-infrared light-emitting diodes (NIR-LEDs; 750–1400 nm of wavelengths) have been implemented into smartphones, proximity sensing, automotive gesture recognition, light detection and ranging (LIDAR) systems for self-driving cars, and virtual reality/augmented reality (VR/AR) headsets for eye-tracking.[4–6] Thus, the IV–VI semiconductor nanocrystals (NCs) such as PbX (X = S, Se) are a focus of special interest owing to their unique intrinsic properties such as narrow band gaps, small effective masses, and large dielectric constants, and IR optoelectronic applications such as IR-LEDs, IR sensors, and array sensors at near-infrared (NIR; 700–1400 nm) and short-wavelength infrared (1400–3000 nm).[7–10] The quantized electronic transition in PbX NCs has been reported to provide size-tunable interband absorption and fluorescence emission at a broad and technically important IR wavelength range, spanning 700–4000 nm.[11–13] Sharp exciton absorption features, high photoluminescence (PL) quantum yield (QY $\sim$ 30%–60%), and high monodispersity ($<$ 5%) of colloidal PbX NCs have been reported.[14–17] They have been extensively explored for fundamental studies, and incorporated into solar cells and IR-LEDs.[8,18–25] Nevertheless, PbSe NC devices have received less attention than their sibling material PbS NC devices mainly due to more problematic air stability. PbSe NCs exhibit spontaneous and irreversible PL peak blue shifting, accompanied by reduction in QY, over a period of days when stored in air.[26–28] The oxidation is ascribed to be the main physical reason. To avoid oxidation and increase stability, the growth of protective shell of a more stable material onto the surface of PbSe NCs has been extensively investigated along with PbS NCs. The synthetic efforts resulted in the synthesis of PbSe/CdSe core/shell NCs via partial cation exchange,[29] and epitaxial grown PbSe/PbS and PbSe/PbSe$_x$S$_{1-x}$ core/shell NCs.[30] The former relies on the shell growth proceeding through the gradual replacement of Pb cations by newly introduced cations in solution and anion sublattice, accompanying the decrease of the PbX core. Noticeable blue shifts of exciton

*Project supported by the National Key Research and Development Program of China (Grant No. 2016YFB0401702), the National Natural Science Foundation of China (Grant Nos. 61674074 and 61405089), Development and Reform Commission of Shenzhen Project, China (Grant No. [2017]1395), Shenzhen Peacock Team Project, China (Grant No. KQTD2016030111203005), Shenzhen Key Laboratory for Advanced Quantum Dot Displays and Lighting, China (Grant No. ZDSYS201707281632549), Guangdong Province's Key R&D Program: Micro-LED Display and Ultra-high Brightness Micro-display Technology, China (Grant No. 2019B010925001), Guangdong University Key Laboratory for Advanced Quantum Dot Displays and Lighting, China (Grant No. 2017KSYS007), and Distinguished Young Scholar of National Natural Science Foundation of Guangdong, China (Grant No. 2017B030306010). We thank the start-up fund from Southern University of Science and Technology, Shenzhen, China.

†Corresponding author. E-mail: sunxw@sustech.edu.cn

peak in the absorption and emission spectra were observed after the cation exchange. The latter is performed by overgrowing wider band gap PbS shells onto PbSe cores, i.e., by exposing the core NCs to all the precursors of the shell elements. Thus, the core size remains essentially constant during the overcoating process. These core/shell NCs provide better air stability by the shell protecting the PbSe core. For PbSe/CdSe core/shell NCs, the excited electrons are partially delocalized into the CdSe shell,[29] while the large valence band offset between PbSe[18,31] and CdSe[32] effectively confines the excited holes to the PbSe core as seen in Fig. 1(a). For PbSe/PbS, and PbSe/PbSe$_x$S$_{1-x}$ core/shell NCs, the electrons are considered to be confined in the core, while the holes are delocalized over the entire core–shell heterostructures in Fig. 1(b).[18,19,33,35] Interestingly, the theoretical calculation by using $k \cdot p$ theory on the PbSe/PbS core/shell NC showed that the electron and hole wavefunctions spread out over the entire core/shell structure and their energy levels are determined by the total diameter of the PbSe/PbS NCs.[33] The PbSe/CdSe and PbSe/PbS core/shell NCs are classified as a so-called quasi-type II heterostructure system. In this type of heterostructure, one carrier is delocalized over the entire NC, while the other is confined in either the core or the shell. Thus, with a single shell layer such as CdSe, PbS, and PbSe$_x$S$_{1-x}$, the NC surface still remains accessible to the charges and thus, the NCs are not fully isolated from their environment.

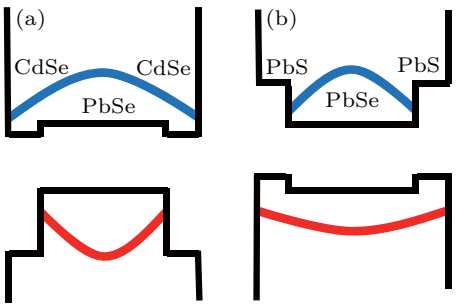

Fig. 1. Schematic illustration of the energy band diagrams with possible electron (blue line) and hole (red line) wavefunctions for (a) PbSe/CdSe core/shell NCs and (b) PbSe/PbS core/shell NCs.

Recently, a quasi-type-II thick-shell CdSe/CdS system demonstrated the benefits of both suppressed blinking and Auger recombination due to a combination of size and carrier separation.[36,37] The ability to simultaneously suppress blinking and nonradiative Auger recombination has important implications for optoelectronic applications such as LEDs[38,39] and low-threshold lasing.[40] Thus, the development of synthetic routes for PbX NCs with thick-shell is very desirable for IR optoelectronic applications. Most works in the literature related to PbSe/CdSe and PbSe/PbS core/shells NCs showed relatively thin shells $\sim\leq$ 1 nm.[29,30,41] Growing thick shells is much less explored for PbX NCs, even though they have uniquely important technological benefits in LEDs and solar cells by suppressing the Auger recombination.[36] Visible LEDs fabricated with CdSe/CdS core/shell NCs demonstrated clearly that thicker shell NCs improve the device performance by about one order of magnitude compared to thinner shell NCs.[42] Recently, for growing a shell thickness $>$ 2 nm, PbSe/CdSe core/shell NCs through cation exchange[43] and PbS/CdS/CdSe core/shell/shell NCs via nano-shell deposition method were explored, and the dual emission in the infrared and visible was observed from the core and the shell, respectively, which may not be the ideal structure for IR device applications. Compared to the CdX shells, PbS is considered a good candidate for a shell material because both PbSe and PbS possess the same rock-salt crystal structure and similar crystallographic parameters, resulting in a small lattice mismatch ($\sim$ 3%; 6.12 Å and 5.94 Å for bulk PbSe and PbS, respectively[44]). The PbSe/PbS core/shell NCs with the shell thickness of 1.8 nm were synthesized by the Lifshitz group and excellent stability in air exposure was reported.[30]

Motivated by these initial results, here, we report on the synthesis and characterization of the PbSe/PbS core/shell NCs by using a syringe pump shelling method and the device characterization of IR-LEDs.[41,45] Two syringe pumps are used for the injection of Pb precursors (Pb-oleate) and S precursors (TMS-S, the mixture of hexamethyldisilathiane (TMS) and 1-octadecene (ODE)), which allows us to control the molecular ratio of Pb and S by adjusting the injection rate of either pump, as to reach the desired quality for the final products. The concentration of PbSe NC in toluene is determined by measuring the absorbance at 400 nm and by using the extinction coefficient of the PbSe NCs (see details in the supporting information).[46]

2. Results and discussion

Absorption and photoluminescence (PL) spectra of the PbSe core NCs and PbSe/PbS core/shell NCs with varying reaction time of 7 min, 15 min, 20 min, and 25 min are shown in Fig. 2(a). The exciton peak of the core PbSe NCs is located at 1200 nm and their diameter is estimated as 3.7 nm by using an empirical equation for the size dependence of the energy gap: $E_g = 0.28 + 4.43d^{-1.34} + 0.555d^{-4.62}$,[47] where the energy gap E_g is expressed in units of eV and NC diameter d in nm. The systematic shift of the exciton peak to the longer wavelength in the absorption as well as emission spectra is clearly observed with increasing reaction time, indicating PbS shell growth. From the TEM image in Fig. 1(b), the physical diameter of the PbSe core is estimated to be 3.5 nm, which agrees with the diameter obtained from the empirical equation. The TEM images of the PbSe/PbS core/shell NCs with reaction time of 15 min and 25 min in Fig. 1(b) also show the growth of the PbS shell. The diameters of the PbSe/PbS core/shell NCs are estimated to 3.9 nm, 4.8 nm, 5.3 nm, and 6.8 nm for the reaction time of 7 min, 15 min,

20 min, and 25 min, respectively. Thus, the thickness of their PbS shell varies from 0.2 min to 1.7 nm with increasing reaction time. The corresponding PLQYs decrease from 25% for PbSe core NCs to 22.5%, 9.4%, and 10.5% for PbSe/PbS core/shell NCs with the reaction time of 7 min, 15 min, and 20 min, respectively. The red-shift of the excitonic transition can be explained by a relatively larger conduction band offset (~ 0.155 eV) for electrons and a smaller valence band offset originated from the small energy difference of bulk PbS and PbSe (~ 0.025 eV),[48] leading to the delocalization of holes. The Stokes shifts and full widths at half maximum (FWHMs) of the absorption and emission peaks obtained from fitting using a single Gaussian function decrease during the reaction as the PbS shell grows (see Fig. S1 in the supporting information), which are consistent with the reports from the Lifshitz group.[41,49] It is interesting to point out that the PbSe/PbS core/shell NCs ($\lambda_{ex} \sim 1600$ nm) with a thickness of 1.8 nm PbS shell from the Lifshitz group showed about 200-nm red shift of the exitonic transition compared to the starting PbSe core NCs ($\lambda_{ex} \sim 1400$ nm).[30] However, as seen in Fig. 2, the PbSe/PbS NCs with reaction time of 25 min have a red shift of 606 nm, even though the PbS shell thickness is estimated as 1.7 nm from their TEM images, i.e., they show a 3 times larger shift of the exciton transition by growing a similar PbS shell. It may require a further study to understand the difference. Further, the exciton peak of the PbSe/PbS core/shell CQDs has nearly the same position for at least 5 days (see the supporting information), indicating better chemical stability of the PbSe/PbS core/shell NCs compared to PbSe core NCs.

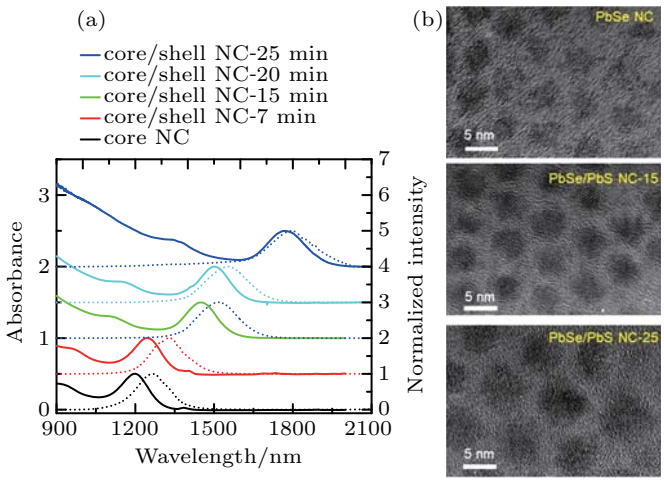

Fig. 2. (a) Absorption (solid lines) and emission (dotted lines) spectra of PbSe core (black) and PbSe/PbS core/shell NCs with reaction time of 15 min (red) and 25 min (blue). A red shift of the exciton peak with an increase of the reaction time is clearly observed. (b) Typical TEM images of PbSe core NCs (top) and PbSe/PbSe core/shell NCs with the reaction time of 15 min (middle) and 25 min (bottom). Their sizes are estimated to 3.5 nm, 4.8 nm, and 6.8 nm, respectively. The scale bars are 5 nm.

For epitaxially growing PbS shells, it is important to control the sulfur concentration below the nucleation threshold.[15] In our synthesis, the sulfur concentration is kept below 100 mM. The molar ratio of Pb and S is also critical for efficient PbS layer growth. Higher molar ratios of Pb/S (> 2) lead to the relatively slow growth of the PbS shell (see Figs. S2 and S3 in the supporting information). With the lower concentration of PbSe NCs (< 10 mg/mL), another emission peak appears with longer reaction time (> 10 min), which is lower than the excitonic emission peak (see Fig. S3 in the supporting information). This may originate from the nucleation by Pb and S precursors or uneven PbS shell growth.

To study radiative lifetimes and LED performance, relatively small PbSe core and PbSe/PbS core/shell NCs are used due to the limited detection wavelength of our InGaAs detector for PL lifetime measurements ($\lambda_{cutoff} = 1350$ nm). Thus, another batch of PbSe/PbS core/shell NCs were synthesized with the small-sized PbSe NCs having the exciton peak at 1021 nm (diameter of 3.2 nm) and the emission peak at 1144 nm. These samples allowed us to measure the QYs and PL lifetimes, and to characterize the fabricated IR-LEDs together. Figure 3(a) shows the absorption and emission spectra of the core PbSe and core/shell PbSe/PbS NC with the reaction time of 10 min. The 112-nm red-shift of the excitonic transition of the PbSe/PbS core/shell NCs is observed and their emission peak is located at 1280 nm. The corresponding QYs are measured to be 29% and 23%, respectively.

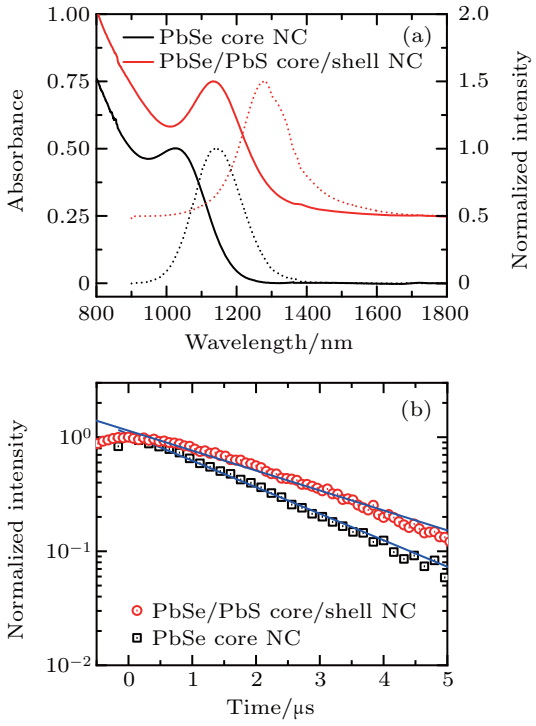

Fig. 3. (a) Absorption (solid lines) and emission (dotted lines) spectra of the small-sized PbSe core and PbSe/PbS core/shell NCs. (b) PL decays of the PbSe core NCs (black squares) with the decay constant of 1.9 μs and PbSe/PbS core/shell NCs (red circles) with the decay constant of 2.5 μs. Solid blue lines: fits using single exponential decay functions.

The fluorescence lifetimes of the core PbSe NCs and core/shell PbSe/PbS NCs were measured and fitted nicely with the single exponential decay function. The decay constants

of the core PbSe NCs and PbSe/PbS core/shell NCs are obtained as 1.9 μs and 2.5 μs, respectively, as seen in Fig. 3(b). PL lifetimes in the microsecond range have been reported in prior studies of colloidal lead-salt NCs.[19,50] It is interesting that the PbSe/PbS core/shell NCs have a longer lifetime. It is well-known that PL lifetimes become shorter and QYs decrease when the size of lead-salt NCs increases.[51,52] This phenomenon has been explained by the strong coupling of exciton to the vibrational modes of capping ligands of NCs.[51–53] Thus, when the electronic state in NCs with increasing NC sizes are closer to the vibration modes of ligands, typically C–H and N–H modes ∼ 3330 nm, the resonant energy transfer for intraband relaxation[54,55] could work as stronger nonradiative decay channels. Thus, the longer PL lifetime of the PbSe/PbS NCs is a counterintuitive phenomenon. However, this longer PL lifetime can be explained by considering the energy level structure of the PbSe/PbS core/shell NCs. Unlike the core-only and type-I systems, in type-II (carriers spatially separated) heterostructures, the electron–hole wavefunction overlap is reduced and even repulsive Coulomb interactions can be developed.[56] Thus, this decreased spatial overlap causes longer PL decay times and the reduction of QYs with the increased shell thickness.[32,57,58] The increased PL lifetime of the PbSe/PbS core/shell NCs can be explained by the increasing delocalization of the hole wave function with increasing shell thickness leading to the decrease of the square of electron–hole overlap integral. Our result agrees with the observation of longer radiative lifetimes of the PbSe/PbS core/shell NCs compared to those of the corresponding cores.[59]

The PbSe/PbS core/shell NCs described in Fig. 3 are used to fabricate IR-LEDs on a prepatterned indium-doped tin oxide (ITO)-coated glass substrate using solution processing and surface treatment. The original oleic acid ligands from the NCs are exchanged in film using mercaptooctanoic acid (MOA) ligands, which have been used to yield a high radiative recombination rate within the active layer by adjusting the spacing between NCs.[8] The $CdCl_2$ treatment is followed after the MOA-ligand exchange, which has been reported to enhance the chemical stability of PbSe NCs against oxidation and increase PLQYs by passivating defects.[60–62] The LED architecture is inspired by prior studies with PbS NC-LEDs (organic–NC–inorganic hybrid), which have shown high efficiency.[22] Figure 4(a) shows the schematic structure of the fabricated devices consisting of a ZnO nanoparticle (NP) electron-transporting layer (ETL) and an organic small molecule hole-transporting layer (HTL) of 4,4-bis(carbazole-9-yl)biphenyl (CBP), sandwiching a film of NCs in an inverted device architecture. Thin films of ITO, gold (Au), and molybdenum trioxide (MoO_3) serve as the cathode, anode, and hole-injection layers, respectively.[63,64] An energy level diagram of the PbSe/PbS core/shell NC-LEDs is shown in Fig. 4(b).[18,22]

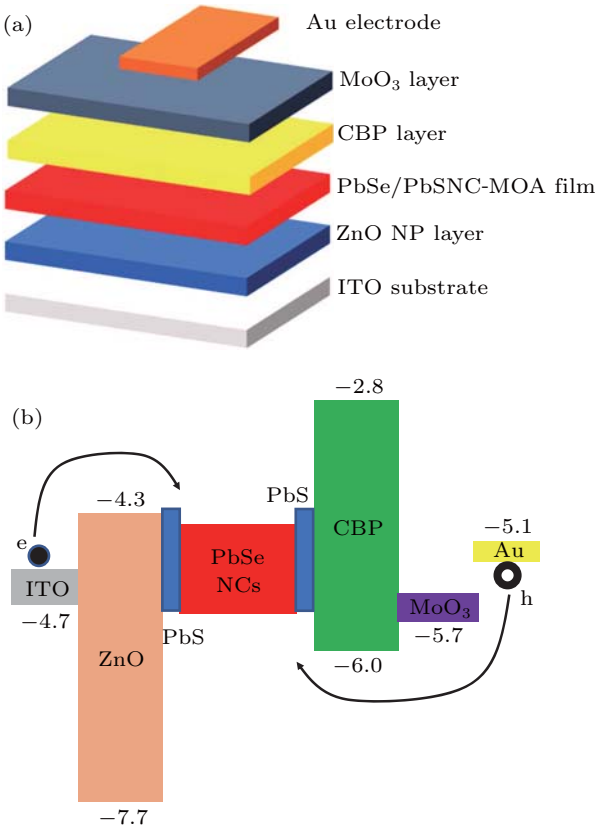

Fig. 4. Device structure. (b) The energy level diagram of the PbSe/PbS NC-LEDs.

Figure 5(a) exhibits the PL spectrum (black line) of the PbSe/PbS NCs in tetrachloroethylene (TCE), and electroluminescence (EL) spectra of MOA-capped (red line) and MOA-capped/Cl-treated (blue line) PbSe/PbS NC-LEDs. The peak positions of the EL spectra match well with the PL spectrum, except that in the EL spectra, their spectral linewidth and line shape are wider and more asymmetric. The broadening of linewidth and the change of line shape from PL to EL can be attributed to the deep traps at the surface of the NCs. The recent study showed that emission from individual PbS NCs arises from a pinned-charge defect state and a band-edge state leading to the PL asymmetry.[65] It is also expected that the emission of the PbSe NCs originates from defects and a band-edge state due to similar optical properties of both NC materials. Thus, it is likely that the MOA-ligand exchange modifies the surface of the PbSe/PbS core/shell NCs and generates the deep trap states at the surface of the NCs, which lead to the asymmetric shape and broadening of the emission peak. In addition, the similar EL shape in MOA-capped and MOA-capped/Cl-treated devices with the slightly broadened EL spectrum of the MOA-capped/Cl-treated device leads us to conclude that the Cl-treatment does not provide adequate surface passivation for the deep traps after a MOA ligand exchange though the stability of PbSe/PbS NC film was quite

enhanced. After the device characterizations in ambient condition, the MOA-capped PbSe/PbS NC-LEDs degraded quickly in less than one day. On the other hand, the Cl-passivated devices lasted up to two days though the device performance was quite lower. Therefore, the Cl-treatment seems to have limited effect on the MOA-capped devices.

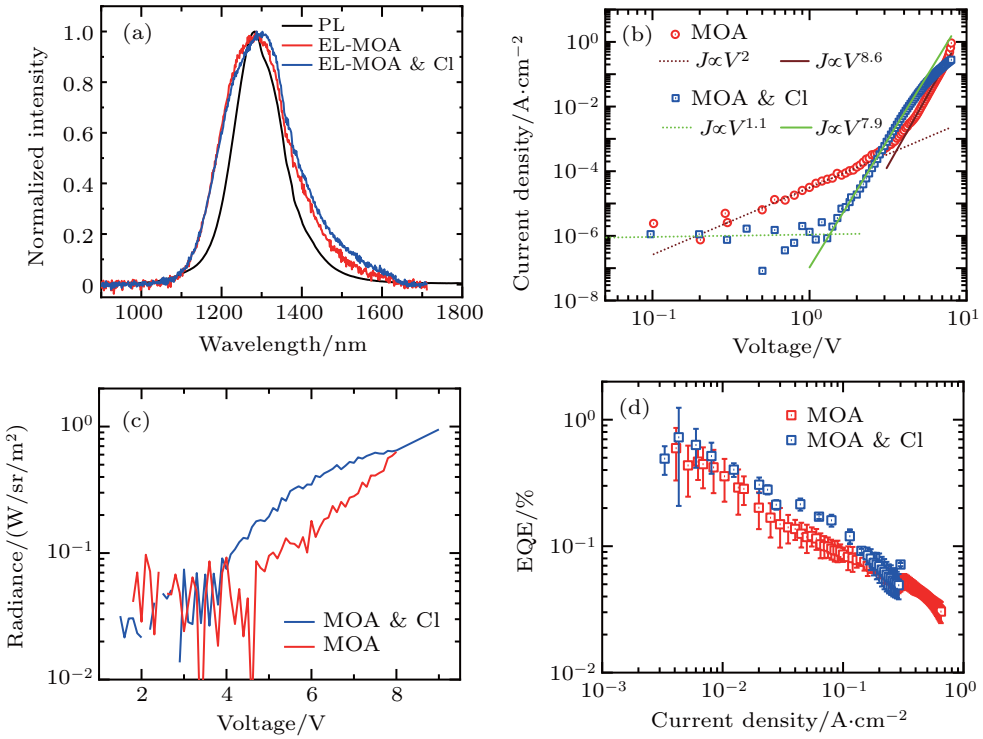

Fig. 5. (a) PL (black line) spectrum of PbSe/PbS NCs in TCE and EL spectra of MOA-capped (red line) and MOA/Cl-treated (blue line) devices. (b) Electrical characteristics of MOA-capped (red circles) and MOA/Cl-treated (blue circles) devices. Fitted results are displayed by the wine lines for MOA-capped devices and by green lines for MOA/Cl-treated devices. (c) Radiance–voltage characteristics of these devices. (d) External quantum efficiency–current density performance of these devices. Error bars indicate the standard deviation of device-to-device variations.

Figure 5(b) shows the typical current density–voltage (J–V) behaviors for both MOA-capped (red circles) and MOA-capped/Cl-treated (blue squares) PbSe/PbS NC-LEDs. In the MOA-capped/Cl-treated NC-LEDs, the current density increases linearly with voltage below 2 V, i.e., the Ohmic regime: $J \propto V$ (dotted green line) and then, enters a trap-limited space-charge conduction regime, which can be fitted by $J \propto V^{7.9}$ (solid green line) according to the Mott–Gurney equation.[66–68] This is consistent with the electrical characteristics of PbS core and PbS/CdS core/shell NC-LEDs having the similar device structure.[22] Interestingly, the J–V characteristics of the MOA-capped NC-LEDs is fitted well by $J \propto V^2$ at low voltages ($V < 3$ V) (dotted wine line), implying that the current is the space-charge limited (SCL). It could be explained by a result of filling all the traps at low voltages. However, at higher voltages, it can be seen that the voltage dependence of current, $J \propto V^{8.6}$ (solid wine line), exhibits the SCL behavior with traps again. Now the physical mechanisms about the different dependence at low voltages is unclear. Further studies are required to understand this behavior.

The effect of the Cl-treatment on MOA-capped NC-LEDs can be clearly observed in Figs. 5(c) and 5(d). The radiance–voltage plot in Fig. 5(c) shows that the Cl-passivation results in a reduction in turn-on voltage from 5 V to 4 V. This may be due to more efficient NC charge injection by reducing partially the deep traps at the surface of the PbSe/PbS core/shell NCs from the MOA treatments. Besides, the breakdown voltage of the devices is improved from 8 V to 9 V by the Cl-passivation as seen in Fig. 5(c). However, the turn-on voltages are still much higher than those of PbS NC-based LEDs (1.4–2 V) having similar device structure.[22] The energy barriers for electron and hole injection of our devices should be lower than those of PbS NC-based LEDs under the similar platform due to the lower LUMO and HOMO levels of the PbSe core and PbSe/PbS NCs (see Fig. S5 in the supporting information).[18,19,49] It could be attributed to a result of the high barriers of the surface states induced by the MOA ligand exchange. The presence of any surface states could be influential in determining the voltage required for electron and hole injection from the ETL and HTLs.

The external quantum efficiency (EQE)–current density data are shown in Fig. 5(d). The MOA-capped and MOA-capped/Cl-treated PbSe/PbS core/shell NC-LEDs exhibit average EQEs of $0.6 \pm 0.26\%$ with a peak EQE of 1% and $0.73 \pm 0.52\%$ with a peak EQE of 1.3%, respectively. EQE–current density has the power-law dependence such as EQE $\propto J^{-0.6}$ with different coefficients. In our knowledge, these are the best performance from PbSe NC-based IR-LEDs.[69,70] The

performance of our PbSe/PbS core/shell NC-LEDs is worse than that of the recent PbS NC-based IR-LEDs with EQEs of 4–8%[22,23,25] but it is not far behind. Besides, it should be noted that due to the detector limitation of our EQE setup, the EL spectra could not be measured with the current density less than 5×10^{-2} A/cm^2. Recent high EQEs of PbS NC-based IR-LEDs were measured at the current densities of 10^{-3}–10^{-4} A/cm^2 and our device area (4 mm^2) is slightly larger than that ($\sim$ 3.1 mm^2) of the reported PbS NC-based IR-LEDs.[8,23,25] Taking into account these two factors, the peak EQEs of our PbSe/PbS core/shell NC-LEDs could reach higher EQEs such as $\sim$ 3% in the current densities of 10^{-3}–10^{-4} A/cm^2 (see the fitted result in Fig. S6 in the supporting information). Further, the current device platform may not be the optimal structure for PbSe NC-based LEDs. Considering that no attempt was made to optimize the performance, the results are encouraging, and we expect that significant improvement can be made.

The ligand exchange and the shell in the PbSe NC-based LEDs play important roles in device performance due to the optimized inter-distance between NCs and the enhanced chemical stability to oxidation. The fabricated devices without MOA-ligand exchange did not emit light even though the previous IR-LEDs with PbS core and PbS/CdS core/shell NCs exhibited good device performance without a ligand exchange under the similar device structure.[22] It may be attributed to the use of thicker NC layer in our devices ($\sim$ 20 nm) due to the higher surface roughness of the ZnO NP layer ($d_{\mathrm{ZnO}} = 4$–5 nm). In addition, the PbSe NC film is quickly oxidized during the MOA ligand exchange in the glove box.

One advantage of PbSe/PbS NCs over their siblings PbS or PbS/CdS NCs on IR-LEDs is that no charge transfer is expected from most PbSe or PbSe/PbS NCs to the metal oxide ETLs such as ZnO, TiO_2, and SnO_2 due to the lower LUMO levels of the PbSe core and PbSe/PbS core/shell NCs ($d_{\mathrm{NC}} > 4$ nm) compared to the conduction band of the metal oxides.[18,49] On the other hand, the charge transfer from PbS or PbS/CdS NCs to metal oxides layers including ZnO is expected when their sizes are smaller than 10 nm[19,22] (see the energy level diagram of PbS and PbSe NCs, and ZnO in Fig. S5 of supporting information).

3. Conclusions

In summary, the PbSe/PbS core/shell/ NCs showing wide optical tunability (from 1200 nm to 1772 nm) are successfully synthesized by controlling the reaction time and molar ratio of Pb and S precursors. We employ the PbSe/PbS NCs in hybrid organic-NC-inorganic LEDs, and the best performance is achieved using MOA-capped/Cl-treated PbSe/PbS NCs. A peak EQE of 1.3% with an average EQE of 0.73% at 1280 nm is the highest number among PbSe NC-based IR-LEDs. Our results demonstrate that the PbS shell is critical for better chemical stability in PbSe NC-based LEDs, along with the improved radiative recombination by the optimized inter-distance between NCs. We believe that further optimization work will improve the device performance and reach comparable performance to that of PbS NC-based IR-LEDs.

Supporting information available

Description of NC synthesis, optical characterizations, and fabrication of LEDs, and additional data analysis are provided in the supporting information.

Acknowledgment

The authors would like to thank the Pico Center at SUSTech that receives support from Presidential fund.

References

[1] Agis F G, Heide S V D, Okonkwo C, Tangidongga E and Koonen T 2017 43*th European Conference on Optical Communication*, September 17–21, 2017, Gothenburg, Sweden, p. 1
[2] Sousa E, Vardasca R, Teixeira S, Seixas A, Mendes J and Costa-Ferreira A 2017 *Phys. Technol.* **85** 315
[3] Willer U, Saraji M, Khorsandi A, Geiser P and Schade W 2006 *Opt. Lasers Eng.* **44** 699
[4] Ionescu B, Suse V, Gadea C, Solomon B, Ionescu D, Islam S and Cordea M 2014 *IEEE Lat. Am. Trans.* **12** 520
[5] Thakur R 2018 *Recent Development in Optoelectronic Devices* (Rijeka: IntechOpen) ED1 - Ruby Srivastava 2018, (Rijeka: IntechOpen) pp. 81–83
[6] Lee W O, Lee H C, Cho C W, Gwon S Y, Park K R, Lee H and Cha J 2012 *Opt. Express* **51** 1
[7] Wise F W 2000 *Acc. Chem. Res.* **33** 773
[8] Sun L, Choi J J, Stachnik D, Bartnik A C, Hyun B R, Malliaras G G, Hanrath T and Wise F W 2012 *Nat. Nanotechnol.* **7** 369
[9] Konstantatos G, Howard I, Fischer A, Hoogland S, Clifford J, Klem E, Levina L and Sargent E H 2006 *Nature* **442** 180
[10] Rauch T, Böberl M, Tedde S F, Fürst J, Kovalenko M V, Hesser G, Lemmer U, Heiss W and Hayden O 2009 *Nat. Photon.* **3** 332
[11] Murray C, Sun S, Gaschler W, Doyle H, Betley T and Kagan C 2001 *IBM J. Res. Dev.* **45** 47
[12] Hines M A and Scholes G D 2003 *Adv. Mater.* **15** 1844
[13] Pietryga J M, Schaller R D, Werder D, Stewart M H, Klimov V I and Hollingsworth J A 2004 *J. Am. Chem. Soc.* **126** 11752
[14] Weidman M C, Beck M E, Hoffman R S, Prins F and Tisdale W A 2014 *ACS Nano* **8** 6363
[15] Lee J W, Kim D Y, Baek S, Yu H and So F 2016 *Small* **12** 1328
[16] Campos M P, Hendricks M P, Beecher A N, Walravens W, Swain R A, Cleveland G T, Hens Z, Sfeir M Y and Owen J S 2017 *J. Am. Chem. Soc.* **139** 2296
[17] Čapek R K, Yanover D and Lifshitz E 2015 *Nanoscale* **7** 5299
[18] Choi J J, Lim Y F, Santiago-Berrios M B, Oh M, Hyun B R, Sun L, Bartnik A C, Goedhart A, Malliaras G G, Abruña H D, Wise F W and Hanrath T 2009 *Nano Lett.* **9** 3749
[19] Hyun B R, Zhong Y-Wu, Bartnik A C, Sun L, Abruña H D, Wise F W, Goodreau J D, Matthews J R, Leslie T M and Borrelli N F 2008 *ACS Nano* **2** 2206
[20] Hyun B R, Choi J J, Seyler K L, Hanrath T and Wise F W 2013 *ACS Nano* **7** 10938
[21] Kim G H, García de Arquer F P, Yoon Y J, Lan X, Liu M, Voznyy O, Yang Z, Fan F, Ip A H, Kanjanaboos P, Hoogland S, Kim J Y and Sargent E H 2015 *Nano Lett.* **15** 7691
[22] Supran G J, Song K W, Hwang G W, Correa R E, Scherer J, Dauler E A, Shirasaki Y, Bawendi M G and Bulović V 2015 *Adv. Mater.* **27** 1437
[23] Gong X, Yang Z, Walters G, Comin R, Ning Z, Beauregard E, Adinolfi V, Voznyy O and Sargent E H 2016 *Nat. Photon.* **10** 253
[24] Yang X, Ren F, Wang Y, Ding T, Sun H, Ma D and Sun X W 2017 *Sci. Rep.* **7** 14741

[25] Pradhan S, Di Stasio F, Bi Y, Gupta S, Christodoulou S, Stavrinadis A and Konstantatos G 2019 *Nat. Nanotechnol.* **14** 72

[26] Dai Q, Wang Y, Zhang Y, Li X, Li R, Zou B, Seo J, Wang Y, Liu M and Yu W W 2009 *Langmuir* **25** 12320

[27] Leschkies K S, Kang M S, Aydil E S and Norris D J 2010 *J. Phys. Chem. C* **114** 9988

[28] Chappell H E, Hughes B K, Beard M C, Nozik A J and Johnson J C 2011 *J. Phys. Chem. Lett.* **2** 889

[29] Pietryga J M, Werder D J, Williams D J, Casson J L, Schaller R D, Klimov V I and Hollingsworth J A 2008 *J. Am. Chem. Soc.* **130** 4879

[30] Brumer M, Kigel A, Amirav L, Sashchiuk A, Solomesch O, Tessler N and Lifshitz E 2005 *Adv. Funct. Mater.* **15** 1111

[31] Jasieniak J, Califano M and Watkins S E 2011 *ACS Nano* **5** 5888

[32] Kim S, Fisher B, Eisler H J and Bawendi M 2003 *J. Am. Chem. Soc.* **125** 11466

[33] Bartnik A C, Wise F W, Kigel A and Lifshitz E 2007 *Phys. Rev. B* **75** 245424

[34] Hyun B R, Zhong Y W, Bartnik A C, Sun L, Abruña H D, Wise F W, Goodreau J D, Matthews J R, Leslie T M and Borrelli N F 2008 *ACS Nano* **2** 2206

[35] Lifshitz E, Vaxenburg R, Maikov G I, Yanover D, Brusilovski A, Tilchin J and Sashchiuk A 2011 (Cambridge: Elsevier) p. 181

[36] García-Santamaría F, Chen Y, Vela J, Schaller R D, Hollingsworth J A and Klimov V I 2009 *Nano Lett.* **9** 3482

[37] Chen Y, Vela J, Htoon H, Casson J L, Werder D J, Bussian D A, Klimov V I and Hollingsworth J A 2008 *J. Am. Chem. Soc.* **130** 5026

[38] Anikeeva P O, Madigan C F, Halpert J E, Bawendi M G and Bulovic V 2008 *Phys. Rev. B* **78** 085434

[39] Bae W K, Park Y S, Lim J, Lee D, Padilha L A, McDaniel H, Robel I, Lee C, Pietryga J M and Klimov V I 2013 *Nat. Commun.* **4** 2661

[40] Lim J, Park Y S and Klimov V I 2018 *Nat. Mater.* **17** 42

[41] Shapiro A, Jang Y, Rubin-Brusilovski A, Budniak A K, Horani F, Sashchiuk A and Lifshitz E 2016 *Chem. Mater.* **28** 6409

[42] Pal B N, Ghosh Y, Brovelli S, Laocharoensuk R, Klimov V I, Hollingsworth J A and Htoon H 2012 *Nano Lett.* **12** 331

[43] Lin Q, Makarov N S, Koh W, Velizhanin K A, Cirloganu C M, Luo H, Klimov V I and Pietryga J M 2015 *ACS Nano* **9** 539

[44] Delin A, Ravindran P, Eriksson O and Wills J M 1998 *Int. J. Quantum. Chem.* **69** 349

[45] Chen O, Zhao J, Chauhan V P, Cui J, Wong C, Harris D K, Wei H, Han H S, Fukumura D, Jain R K and Bawendi M G 2013 *Nat. Mater.* **12** 445

[46] Moreels I, Lambert K, De Muynck D, Vanhaecke F, Poelman D, Martins J C, Allan G and Hens Z 2007 *Chem. Mater.* **19** 6101

[47] Bartnik A C 2011 *The Dependence Of Lead-Salt Nanocrystal Properties On Morphology And Dielectric Environment* (Ph.D. Dissertation) (Ithaca: Cornell University)

[48] Sashchiuk A, Yanover D, Rubin-Brusilovski A, Maikov G I, Čapek R K, Vaxenburg R, Tilchin J, Zaiats G and Lifshitz E 2013 *Nanoscale* **5** 7724

[49] Jang Y, Shapiro A, Isarov M, Rubin-Brusilovski A, Safran A, Budniak A K, Horani F, Dehnel J, Sashchiuk A and Lifshitz E 2017 *Chem. Commun.* **53** 1002

[50] Wehrenberg B L, Wang C and Guyot-Sionnest P 2002 *J. Phys. Chem. B* **106** 10634

[51] Liu H and Guyot-Sionnest P 2010 *J. Phys. Chem. C* **114** 14860

[52] Semonin O E, Johnson J C, Luther J M, Midgett A G, Nozik A J and Beard M C 2010 *J. Phys. Chem. Lett.* **1** 2445

[53] Lifshitz E 2015 *J. Phys. Chem. Lett.* **6** 4336

[54] Guyot-Sionnest P, Wehrenberg B and Yu D 2005 *J. Chem. Phys.* **123** 074709

[55] Aharoni A, Oron D, Banin U, Rabani E and Jortner J 2008 *Phys. Rev. Lett.* **100** 057404

[56] Nanda J, Ivanov S A, Achermann M, Bezel I, Piryatinski A and Klimov V I 2007 *J. Phys. Chem. C* **111** 15382

[57] Hatami F, Grundmann M, Ledentsov N N, Heinrichsdorff F, Heitz R, Böhrer J, Bimberg D, Ruvimov S S, Werner P, Ustinov V M, Kop'ev P S and Alferov Zh I 1998 *Phys. Rev. B* **57** 4635

[58] Dennis A M, Mangum B D, Piryatinski A, Park Y S, Hannah D C, Casson J L, Williams D J, Schaller R D, Htoon H and Hollingsworth J A 2012 *Nano Lett.* **12** 5545

[59] Yanover D, Vaxenburg R, Tilchin J, Rubin-Brusilovski A, Zaiats G, Čapek R K, Sashchiuk A and Lifshitz E 2014 *J. Phys. Chem. C* **118** 17001

[60] Bae W K, Joo J, Padilha L A, Won J, Lee D C, Lin Q, Koh W, Luo H, Klimov V I and Pietryga J M 2012 *J. Am. Chem. Soc.* **134** 20160

[61] Zhang J, Gao J, Church C P, Miller E M, Luther J M, Klimov V I and Beard M C 2014 *Nano Lett.* **14** 6010

[62] Marshall A R, Young M R, Nozik A J, Beard M C and Luther J M 2015 *J. Phys. Chem. Lett.* **6** 2892

[63] Wang Z B, Helander M G, Qiu J, Liu Z W, Greiner M T and Lu Z H 2010 *J. Appl. Phys.* **108** 024510

[64] Wang Z B, Helander M G, Qiu J, Puzzo D P, Greiner M T, Hudson Z M, Wang S, Liu Z W and Lu Z H 2011 *Nat. Photon.* **5** 753

[65] Caram J R, Bertram S N, Utzat H, Hess W R, Carr J A, Bischof T S, Beyler A P, Wilson M W B and Bawendi M G 2016 *Nano Lett.* **16** 6070

[66] Mott N F and Gurney R W 1940 *Electronic Processes in Ionic Crystals* (New York: Oxford University Press) p. 1142

[67] Rose A 1955 *Phys. Rev.* **97** 1538

[68] Hikmet R A M, Talapin D V and Weller H 2003 *J. Appl. Phys.* **93** 3509

[69] Steckel J S, Coe-Sullivan S, Bulović V and Bawendi M G 2003 *Adv. Mater.* **15** 1862

[70] Choudhury K R, Song D W and So F 2010 *Org. Electron.* **11** 23